Kinetic and functional analysis of abundant microRNAs in extracellular vesicles from normal and stressed cultures of Chinese Hamster Ovary (CHO) cells

Jessica Belliveau, [1,2,*] Will Thompson [1,2,*] and Eleftherios Terry Papoutsakis [1,2,3]

[1] Department of Chemical and Biomolecular Engineering, University of Delaware, Newark, Delaware, USA

[2] Delaware Biotechnology Institute, University of Delaware, Newark, Delaware, USA

[3] Department of Biological Sciences, University of Delaware, Newark, Delaware, USA

[*] Jessica Belliveau (ORCID # 0000-0003-3466-6428) and Will Thompson (ORCID #0000-0002-0014-1941) should be considered joint first author

Correspondence: Eleftherios Terry Papoutsakis, 590 Avenue 1743, Newark, DE 19713, USA. E-mail: epaps@udel.edu; Tel: +1-302-831-8376; ORCID # 0000-0002-1077-1277

Abstract:

Chinese hamster ovary (CHO) cells release and exchange large quantities of extracellular vesicles (EVs). EVs are highly enriched in microRNAs (miRs, or miRNAs), which are responsible for most of their biological effects. We have recently shown that the miR content of CHO EVs varies significantly under culture stress conditions. Here, we provide a novel stoichiometric ("per-EV") quantification of miR and protein levels in large CHO EVs produced under ammonia, lactate, osmotic, and age-related stress. Each stress resulted in distinct EV miR levels, with selective miR loading by parent cells. Our data provide a proof of concept for the use of CHO EV cargo as a diagnostic tool for identifying culture stress. We also tested the impact of three select miRs (let-7a, miR-21, and miR-92a) on CHO cell growth and viability. Let-7a—abundant in CHO EVs from stressed cultures—reduced CHO cell viability, while miR-92a—abundant in CHO EVs from unstressed cultures—promoted cell survival. Overexpression of miR-21 had a slight detrimental impact on CHO cell growth and viability during late exponential-phase culture, an unexpected result based on the reported anti-apoptotic role of miR-21 in other mammalian cell lines. These findings provide novel relationships between CHO EV cargo and cell phenotype, suggesting that CHO EVs may exert both pro- and anti-apoptotic effects on target cells, depending on the conditions under which they were produced.

Keywords:

Chinese hamster ovary cells, extracellular vesicles, microparticles, microRNA, ammonia stress, lactate stress, osmotic stress, culture age

1. INTRODUCTION:

Chinese hamster ovary (CHO) cells have long served as mainstays of industrial protein production. Recently, we have found that CHO cells in culture participate in a massive and continuous exchange of extracellular vesicles (EVs) (J. Belliveau & E. T. Papoutsakis, 2022), thus impacting culture performance by a hitherto unknown and unexplored mechanism . EVs are submicron-sized particles enclosed by a lipid bilayer which originate from either multivesicular bodies or the plasma membrane. EVs from multivesicular bodies (known as “exosomes”) are generally smaller in size (50-150 nm), while EVs released from the plasma membrane (known as microparticles or microvesicles) tend to be larger (100-1,000 nm). Released by every cell type, EVs serve as linchpins of intercellular communication, mediating phenotypes of target cells through the delivery of nucleic acid and/or protein cargo (Kao & Papoutsakis, 2019; Raposo & Stoorvogel, 2013; van Niel, D'Angelo, & Raposo, 2018).

In particular, microRNAs (miRs) have been identified as key molecules responsible for EV biological activities (Dellar, Hill, Melling, Carter, & Baena-Lopez, 2022; O'Brien, Breyne, Ughetto, Laurent, & Breakefield, 2020). Most commonly, miRs influence cellular behavior by binding to complementary sequences on longer mRNAs and subsequently inhibiting protein translation or degrading the mRNA (Dellar et al., 2022; O'Brien et al., 2020). Most miRs have multiple mRNA targets and work together to regulate cellular processes and phenotypes; even small changes in miR expression, such as 1.5-fold change, can affect cellular phenotypes (Mestdagh et al., 2009). EVs are loaded with individual miRs and other cargo by a variety of chaperone proteins (Anand,

Samuel, Kumar, & Mathivanan, 2019; Corrado, Barreca, Zichittella, Alessandro, & Conigliaro, 2021; Fabbiano et al., 2020; Leidal & Debnath, 2020).

CHO EVs have only recently garnered significant attention. In particular, we have found that CHO EVs exchange large quantities of RNA cargo between their parent cells (J. Belliveau & E. T. Papoutsakis, 2022; Belliveau & Papoutsakis, 2023). The nature of that cargo, which has been investigated by several groups (Belliveau & Papoutsakis, 2023; Busch et al., 2022; C. Keysberg et al., 2021), is now known to vary significantly as a function of metabolite (ammonia and osmotic) stress (Belliveau & Papoutsakis, 2023). Preliminary proteomic analysis has also been performed on CHO EVs, with large and diverse protein populations observed in both large and small CHO EVs from various phases of culture (C. Keysberg et al., 2021; Kumar et al., 2016). Still, nothing is known about the specific function of CHO EV cargo in culture. In two instances, CHO EVs have been found to promote desirable phenotypes in target cells, with smaller EVs (i.e., “exosomes”) promoting CHO cell growth (Takagi, Jimbo, Oda, Goto, & Fujiwara, 2021) and protecting CHO cells against oxidative stress (Han & Rhee, 2018). However, the EV cargo mediating these phenotypes remains unknown.

From this vantage point, this study provides novel insights into the functions of CHO EV miR cargo in CHO cells, hinting at possible mechanisms for CHO EV bioactivity observed in other studies. Specifically, we provide a unique (for CHO EV research) stoichiometric accounting of miR and protein cargo levels in EVs produced under various stress conditions. We also examine cellular phenotypes mediated by the three highly-abundant miRs: let-7a, miR-21, and miR-92a.

The focus of this work is the larger EVs, often labeled microvesicles or microparticles (MPs),which have been the focus of fewer studies, but which are easier to isolate—a boon for their potential as a diagnostic tool—and capable of carrying larger cargo loads, thus suitable for a broader range of synthetic applications using DNA, RNA, protein, nucleoprotein (such as CRISPR systems) and other organic molecules as payload. Due to challenges in distinguishing the biogenesis of isolated EVs, the more general term of EV is used here and increasingly in the EV field (Thery et al., 2018). In our previous publication (Belliveau & Papoutsakis, 2023) reporting on the microRNome of CHO cells and their EVs, the larger EVs were called MPs, and the smaller EVs were called exosomes. Our previous publications (J. Belliveau & E. T. Papoutsakis, 2022; Belliveau & Papoutsakis, 2023) have provided detailed CHO EV characterization that meets or exceeds the MISEV2018 guidelines from the International Society for Extracellular Vesicles (Thery et al., 2018). Here, we use the same isolation methods as before, expanding our CHO EV characterization by focusing primarily on various miR cargoes and their potential functions in CHO cell culture.

2. MATERIALS AND METHODS:

2.1 Chemicals and reagents

Except where otherwise noted, all chemicals and reagents were obtained from Sigma-Aldrich (St. Louis, MO, USA) or Thermo Fisher Scientific (Waltham, MA, USA).

2.2 CHO cell culture

CHO cells were obtained and cultured as described previously (J. Belliveau & E. T. Papoutsakis, 2022; Belliveau & Papoutsakis, 2023). Briefly, a CHO-K1 cell line expressing the VRC01 antibody was cultured in HyClone ActiPro media (Cytiva, Marlborough, MA, USA) supplemented with 6 mM L-glutamine. Culture occurred in either 125 mL shake flasks (20 mL culture volume) at 120 rpm or 50 mL culture tubes (15 mL culture volume) at 250 rpm. A seeding density of 0.4 x 10^6 cells/mL was employed in each case, and cells were incubated at 37°C in 20% O_2 and 5% CO_2.

Ammonia stress was applied by adding 9 mM ammonium chloride (NH_4Cl) in phosphate-buffered saline (PBS) (pH 7.4) to day 0 of the culture. Lactate stress was applied by adding 10 mM sodium lactate ($NaC_3H_5O_3$) in PBS (pH 7.4) to day 2 of the culture (to coincide with the natural spike in culture lactate concentration). Osmotic effects of the lactate stress were controlled for via an "osmotic control" treatment, wherein 10 mM of sodium chloride (NaCl) in PBS (pH 7.4) was added to day 2 of the culture, such that the culture osmolarity resulting from the added NaCl was 20 mOsm/L. Higher osmotic stress was applied by adding 60 mM sodium chloride (NaCl) in PBS (pH 7.4) to day 0 of the culture, such that the culture osmolarity resulting from the added NaCl was 120 mOsm/L.

2.3 Isolation and quantification of extracellular vesicles

CHO EVs were isolated and characterized as described (J. Belliveau & E. T. Papoutsakis, 2022; Belliveau & Papoutsakis, 2023). As noted, only large CHO EVs (i.e., "CHO MPs") were collected and analyzed for this study. Briefly, CHO cells were pelleted via centrifugation at 180 x g for 4 min. From the resulting supernatant, apoptotic bodies and large cellular debris were pelleted

via centrifugation at 2,000 x g for 10 min. Finally, from this new supernatant, CHO EVs were pelleted via ultracentrifugation at 28,000 x g and 4°C for 30 min. Ultracentrifugation employed an Optima LE-80K Ultracentrifuge with an SW-28 rotor (Beckman Coulter, Brea, CA, USA) for initial separation and an Optima Max Ultracentrifuge with a TLA-55 rotor (Beckman Coulter, Brea, CA, USA) for sample enrichment and washing. Isolated CHO EVs were resuspended in culture media and used immediately or stored at 4°C overnight.

CHO EVs were counted using either a BD FACSAriaII flow cytometer with FACSDiva software (BD Biosciences, Franklin Lakes, NJ, USA) or a CytoFLEX S flow cytometer with CytExpert software (Beckman Coulter, Brea, CA, USA). Here, CHO EVs were defined as all particles between 0.2 micron (the smallest reliable size that can be counted using our flow cytometry instruments) and 1 micron in size; size gates were constructed using fluorescent calibration beads from Spherotech (Lake Forest, IL, USA). For experiments using the BD FACSAriaII flow cytometer, a known quantity of ~5 micron AccuCount Fluorescent Beads (Spherotech, Lake Forest, IL, USA) was used for CHO EV counting.

Further characterization of the CHO EVs including size distribution and protein markers are described in our previous work (Jessica Belliveau & Eleftherios T. Papoutsakis, 2022).

2.4 Extraction of total RNA

Extraction of total RNA from CHO cells and EVs was done as described (Belliveau & Papoutsakis, 2023). Briefly, total RNA was extracted from pelleted cells or EVs using a miRNeasy Mini Kit

(QIAGEN, Hilden, Germany) per manufacturer's instructions. In some cases, a known quantity (1 pmol) of synthetic cel-miR-39-3p (Thermo Fisher Scientific, Waltham, MA, USA) was added to samples during the cell/EV lysis step. This spike-in control enabled the calculation of miRNA copy numbers using the ratio of native miRNA to miR-39 informed by subsequent RT-PCR experiments. Although the same amount of miR-39 was added to each sample, EV input quantity was variable (sample volumes were kept constant). Extracted RNA samples were flash frozen in liquid N_2 and stored at -80°C until further use.

2.6 Quantification of total miR

Total miR levels in extracted RNA samples were quantified using a Qubit miR Assay Kit and Qubit 3.0 Fluorimeter (Thermo Fisher Scientific, Waltham, MA, USA); the manufacturer's protocols were employed.

2.5 Quantification of individual miRs via RT-PCR

Individual miR levels were quantified via RT-PCR as described (Kao, Jiang, Thompson, & Papoutsakis, 2022). Briefly, reverse transcription employed the ThermoFisher TaqMan MicroRNA Reverse Transcription Kit with miR-specific primers and probes (Thermo Fisher Scientific, Waltham, MA, USA), and proceeded according to the manufacturer's protocol. PCR employed the TaqMan Universal PCR Master Mix II with miR-specific Small RNA Assays (Thermo Fisher Scientific, Waltham, MA, USA), and proceeded according to the manufacturer's protocol. For PCR experiments, three technical replicates were performed for each biological replicate. Reverse transcription and PCR used a CFX96 Optical Reaction Module (Bio-Rad, Hercules, CA,

USA), with miR levels quantified via the $2^{-\Delta\Delta CT}$ method (Livak & Schmittgen, 2001). Specifically, the $2^{-\Delta\Delta CT}$ method was used to calculate the ratio of each specific miRNA concentration to the concentration of the spike-in control (miR-39). Because the spike-in control quantity was known, the total copy number of the specific miRNA under investigation could thereafter be calculated and normalized to the total number of EVs used to create the sample.

2.6 Quantification of total protein

Total protein in CHO EV samples was quantified using a Bradford-based, colorimetric assay kit. CHO EVs were washed in PBS and resuspended in RIPA buffer (Millipore Sigma, Burlington, MA, USA) supplemented with protease inhibitor (200:1 buffer-to-inhibitor ratio). Sample volumes ranged from 50 to 300 µL, depending on CHO EV concentration. Samples were agitated at 4°C for 30 min. and thereafter centrifuged at 16,000 x g and 4°C for 25 min. Supernatants containing the total protein were diluted with water (18:2 water-to-lysate ratio). Subsequent protein quantification employed the Bio-Rad protein assay kit (Bio-Rad, Hercules, CA, USA). A 100 µL solution of Reagent A and Reagent S (5:1 ratio) was added to each sample; samples were agitated briefly and incubated at room temperature for 15 min. Absorbance of each sample at 750 nm was recorded for three technical replicates of each biological replicate. A calibration curve was constructed via serial dilution of a BSA standard.

2.7 Plasmid preparation

E. coli transformed with plasmids, detailed below, containing the primary or a fragment of the primary miR sequences were obtained from Addgene as stab cultures, expanded on LB agar

plates with 100 μg/mL carbenicillin, and single colonies were selected to expand in liquid LB cultures with 100 μg/mL carbenicillin overnight. Plasmid purification of the overnight cultures was done with QIAGEN Miniprep Kit (QIAGEN, Hilden, Germany) and quantified with the dsDNA HS Qubit Kit (Invitrogen, Waltham, MA, USA).

2.8 Overexpression of miRs

CHO cells were electroporated with 2 μg of plasmids containing the primary or a fragment of the primary microRNA sequences of three miRs that were in high abundance in standard or stressed cultures (miR-21 (Addgene #21114), miR-92a (Addgene #46672), let-7a (Addgene #51377) using the Nucleofector V kit (Lonza, Basel, Switzerland) according to manufacturer's protocols. Cells were cultured in 2 mL cultures in 12-well plates at 37°C and 120 RPM. Growth media was changed one day after electroporation to remove excess electroporation buffer and 0.2 mg/mL geneticin was added to apply selection pressure to overexpress the plasmids. Geneticin was added every other day to maintain selection pressure. Cell growth was measured every day and viability was measured every other day.

2.9 Viability assay

Viability was measured every other day using an Annexin V (BioLegend, San Diego, CA, USA) and 7AAD (BioLegend, San Diego, CA, USA) flow cytometry assay. Briefly, cells were washed with cold PBS twice, then resuspended in Annexin V Binding Buffer (BioLegend, San Diego, CA, USA) and incubated at room temperature in the dark with FITC-Annexin V (1:20 antibody to binding buffer by volume) and 7AAD (1:20 stain to binding buffer by volume) for 15 minutes.

Cells were then analyzed using flow cytometry (CytoFLEX S flow cytometer using CytExpert Software, Beckman Coulter, Brea, CA, USA).

2.10 Statistical analysis

Except where otherwise noted, each data point represents the mean of ≥3 biological replicates, with error bars indicating ± one standard error of the mean. Unpaired Student's t-tests were performed on all data, with * indicating $p<0.05$, ** indicating $p<0.01$, and *** indicating $p<0.001$.

3. RESULTS:

3.1 Total miR and protein quantities in CHO EVs vary with culture age and stress

Total miR and protein levels in CHO EVs could serve as valuable metrics for CHO culture diagnostics but also for cell-specific miR manufacturing/production. For example, in vitro or in vivo dosages of EVs for biotechnological or therapeutic applications are based on total mass or total proteins, two quantities that are affected by the specific per EV mass or protein. How those might vary with culture parameters has not been systematically reported. Although our prior work has identified individual miR cargo in CHO EVs produced under stress (Belliveau & Papoutsakis, 2023), nothing is known about age/stress-induced variation in total miR or protein levels in CHO EVs. In this study, total miR and protein levels were quantified using Qubit fluorimetry and a Bradford protein assay, respectively. Total miR levels in CHO EVs increased steadily as parent cultures aged, with significant increases in said miR levels occurring from day 3 to day 6 and from day 6 to day 9 (Fig 1a). For CHO EV protein levels, however, the trend was

reversed: levels were highest on day 1 and diminished thereafter, with protein levels dropping significantly from day 3 to day 6 and from day 6 to day 9 (Fig 1b). Notably, total protein weight is much higher than total miR weight at any given point in time. These results were unexpected and surprising in that one would assume that these two EV specific properties are largely constant. The opposite trends (total miR vs total protein) are also unexpected and the mechanism that underlies that is for now unknown.

Total miR levels in CHO EVs were also significantly higher (relative to controls) in day 3 cultures treated with ammonia, lactate, or osmotic (20 and 120 mOsm/L) stress. 120 mOsm/L osmotic stress was also significantly more effective than 20 mOsm/L osmotic stress in boosting total CHO EV miR levels (Fig 2c). However, no level of osmotic stress had an impact on total CHO EV protein levels; only ammonia and lactate stress promoted significant increases in total protein levels (relative to the control) (Fig 2d). In sum, these results suggest that miR and protein loading in CHO EVs is a dynamic process that varies significantly with culture age and stress. While total miR or protein levels are inappropriate as methods for CHO EV counting, they offer promise as metrics for the rapid and non-invasive monitoring of culture stress conditions.

3.2 Levels of highly abundant miRs in CHO cells decrease with culture age

Given the relationship between culture age and CHO EV miR cargo loading, optimal harvest times for CHO EVs with high levels of specific individual miRs must be identified, such that per-EV miR levels are maximized. In this study, RT-PCR was employed to quantify levels of five highly abundant miRs (as determined by RNA sequencing of CHO EVs from standard culture)

(Belliveau & Papoutsakis, 2023). Levels of cgr-miR-92a-3p, cgr-miR-23a-3p, cgr-miR-21-5p, cgr-miR-25-3p, and mmu-let-7c-5p were assessed in both CHO EVs and CHO cells on days 1, 3, 6 and 9 of culture. Highly sensitive TaqMan assays combined with spike-in control cel-miR-39-3p enabled calculation of miR copy number per EV via the $2^{-\Delta\Delta CT}$ method (Livak & Schmittgen, 2001), which is an increasingly popular method for EV miR cargo quantification (Kondratov et al., 2020; Perge et al., 2017). It should be noted that EV count is dependent on the method of counting (e.g. NTA or flow cytometry). Here,EV counting via flow cytometry was used. Cellular levels of all five miRs decreased significantly as cultures aged, with the most significant drops observed between day 3 and day 9 (Fig 2b). Similar decreases were observed between CHO EVs derived from day 1 and day 3 cultures, though these drops were not significant (Fig 2a). We suggest that the high variability in the day 1 EVs is the result of variability during culture startup (i.e., due to inoculum variability). Individual miR levels in CHO EV samples from days 6 and 9 were not detectable via RT-PCR, possibly the result of a co-isolated product inhibiting reverse transcription and/or amplification. Nevertheless, trends in cellular miR levels suggest that CHO EV miR levels may also vary significantly with culture age. Optimization of harvest times for CHO EVs possessing high or low levels of various specific miRs must therefore be a priority.

3.3 Highly abundant individual miRs are more highly enriched in CHO EVs from unstressed cultures, a phenomenon not observed in the parent cells

Levels of the individual miRs noted above were also measured in CHO EVs (Fig 3a) and CHO cells (Fig 3b) produced/grown under osmotic, ammonia, and lactate stress. Samples were taken from day 3 culture, with samples from unstressed cultures serving as controls. Since lactate stress did

not inhibit cell growth, a 20 mOsm/L NaCl control was used to assess whether the impact of lactate on EV miR cargo was due to its osmotic effects. The individual miR levels in CHO EVs from unstressed cultures were, without exception, higher than the levels observed in CHO EVs from stressed cultures, regardless of the type or magnitude of stress, and this trend was statistically significant for miR-25 and let-7c. Notably, despite these relatively large differences between individual miR quantities in stressed and unstressed CHO EVs, miR quantities rarely varied significantly between stressed unstressed parent cells (Fig 3b), suggesting the impact of stress on CHO EV miR levels is mediated not by cellular miR concentrations, but rather by changes in the behavior of protein chaperones responsible for cargo loading (for the five miRs and four stress conditions tested, at least). On the other hand, cellular miR levels under ammonia/lactate stress often were significantly higher than corresponding levels under osmotic stress (Fig 3b), suggesting the various stresses have highly distinct impacts on cellular miR production machinery.

Previous investigations of EVs from other cell types have found abundant miR species to exist in EVs at anywhere from 1 copy per 10–100 EVs (Chevillet et al., 2014; Wei et al., 2017) to 10–100 copies per 1 EV (Kondratov et al., 2020; Stevanato, Thanabalasundaram, Vysokov, & Sinden, 2016). The individual miR copy numbers (per EV) identified in this study fit quite reasonably within these ranges, with especially notable expression (>100 copies) of miR-92a per EV observed in two samples. Traditional flow cytometry is limited in its ability to count particles of less than 200 nm, while nanoparticle tracking analysis (NTA) accounts for smaller particles but is more apt to count non-EV proteins and aggregates (George et al., 2021). For this reason, EV

concentrations are 1-2 orders of magnitude higher when counts are taken via NTA (versus flow cytometry) (George et al., 2021). Given our focus on larger MPs, which are enriched via ultracentrifugation at 28,000 x g, this study counts EVs using flow cytometry.

The RT-PCR data in this section also provide support for a selective CHO EV loading process, both during normal growth and under stress conditions. That is, the miR contents of the CHO EVs are not a proportional reflection of intracellular miR availability, but instead reflect an active, intentional loading process on the part of the parent cell and its protein chaperones. Assuming spherical CHO cells of 15 microns (diameter) and spherical CHO EVs of 250 nm, CHO EVs from unstressed (control) day 3 culture contain volumetric concentrations of miR-92a, miR-21, miR-25, let-7c, and miR-23a that are 5,400, 2,300, 6,800, 18,000, and 6,600 times greater, respectively, than those in their parent cells.

To confirm the validity of our RT-PCR methodology, we used control data (i.e., Fig 2a/3a data from unstressed day 3 culture) to plot miRNA counts per sample versus EV counts per sample for the five abundant miRNAs of interest. As noted in section 2.4, this exercise is possible because sample volume—not total EV input—was kept constant during miRNA extraction. The resulting plots are available in the supplementary material as Fig S1. The obvious linear trends in the data confirm the validity of the method. We suspect that the reason some of the apparent trendlines do not intersect with the origin is because the lower limit of detection for our method is >0 EVs. This limit may be the result of the RT-PCR, but is more likely a

consequence of the RNA extraction procedure, as the TaqMan assay we employ is notoriously sensitive to small amounts of input material.

3.4 Transient overexpression of individual miRs impacts CHO cell growth and viability

Little is currently known regarding the functions of CHO EV miR cargo in target CHO cells. Therefore, we wanted to examine the growth, viability, and apoptosis of CHO cells overexpressing either let-7a, which is highly expressed in CHO EVs from stressed cultures , or miR-21 or miR-92a, both of which are highly expressed in CHO EVs from unstressed, exponential-phase cultures (Belliveau & Papoutsakis, 2023). Let-7a has been reported in the literature to have a negative impact on cell growth and viability in other cell types (Cho, Song, Oh, & Lee, 2015; Tsang & Kwok, 2008; Zhao et al., 2018). On the other hand, miR-21 and miR-92a have been reported to improve cell growth and viability (Feng & Tsao, 2016; Krichevsky & Gabriely, 2009; Liu, Wang, Yang, Xiao, & Chen, 2014; Mogilyansky & Rigoutsos, 2013; Shigoka et al., 2010; Thabet et al., 2020; Xu et al., 2019; Yang et al., 2019; Zhou et al., 2015). In CHO cells, miR-92a has also been shown to boost protein production by raising intracellular cholesterol levels (Loh, Yang, & Lam, 2017).

In this study, cultures were transiently transfected with plasmids encoding miRs that were previously identified to be in high abundance during exponential phase in stressed or standard cultures (let-7a, miR-21, miR-92a) to observe a relationship between these specific miRs and cell growth and viability. We hypothesized overexpressing highly abundant miRs from unstressed cultures identified in exponential phase, miR-21 and miR-92a, throughout the

culture lifespan would promote cell growth and viability, particularly in stationary phase. Conversely, we hypothesized that overexpression of highly abundant miRs from stressed cultures, let-7a, would decrease cell growth and viability. Cultures were compared to a control culture that was transiently transfected with a plasmid encoding a far-red fluorescent protein (pLifeAct-miRFP703) to control for the effects of electroporation, plasmid burden, and selection pressure. The burden of expressing a protein (1 kb) is greater than that of expressing pri-miR sequences (80-150 bp) and, in addition, the expressed protein is a fluorescent reporter that does not have a functional role in the cell. Therefore, the differences in the plasmid effects on cell growth and viability between this control and miR-overexpressing conditions are likely conservative. Another type of control that could have been used is a plasmid with a "random sequence" miR, or an "empty" plasmid (i.e., a plasmid without DNA in the locus of the miR). While widely tested for human miRs, we are concerned that one can never ascertain the a "random sequence" miR has not biological effects in CHO cells for lack of extensive testing. The "empty" option would be preferrable, but in the end we opted for the more conservative pLifeAct-miRFP703 control.

In cultures that were transiently transfected with the let-7a plasmid (Figure 4a), the cell concentrations at days 3, 6, 7, 8, and 9 were significantly lower compared to the control culture, indicating let-7a has a negative impact on cell growth. The cell density of cultures transfected with the plasmid encoding miR-21 was only significantly different from the control culture at days 7 and 8. For cultures with the miR-92a plasmid, the cell density was significantly different from the control on day 2; otherwise, there was no difference in the cell growth curve.

372

373 The viability of these cultures was measured on days 4, 6, and 8 with an annexin V/7AAD flow
374 cytometry assay (Figure 4b). Conditions in red indicate reduced viability or increased apoptosis
375 and conditions in green indicate increased viability or decreased apoptosis compared to the
376 control culture at the same timepoints. On days 4 and 6, cultures transfected with let-7a had
377 significantly fewer viable cells. The let-7a condition had significantly more early apoptotic and
378 late apoptotic cells compared to the control culture, in agreement with reports of let-7a
379 inducing apoptosis (Cho et al., 2015; Tsang & Kwok, 2008).

380

381 Cultures with the plasmid expressing miR-21 demonstrated decreases in the populations of
382 viable and early apoptotic cells and an increase in the population of late apoptotic cells on day
383 6 of culture. miR-21 is highly expressed during exponential phase in normal batch cultures and
384 is reported in other mammalian cell lines to have an anti-apoptotic role and support cell growth
385 (Feng & Tsao, 2016; Krichevsky & Gabriely, 2009); therefore, we initially hypothesized that
386 overexpression of miR-21 through stationary phase would support both cell growth and
387 viability. However, in cultures overexpressing miR-21, a decrease in cell density and a decrease
388 in cell viability was observed during late stationary phase. Our study therefore suggests that the
389 impacts of overexpressing miR-21 by up to twofold on CHO cell growth and viability are
390 negligible in early culture, and may be negative in mid to late culture. Cultures with the plasmid
391 expressing miR-92a demonstrated an increase in the population of viable cells on day 8 of
392 culture compared to the control culture at the same timepoint. In the literature, miR-92a is
393 reported to increase cell proliferation (Zhou et al., 2015), and was observed in our previous

394 experiments to be highly expressed early in culture (Figure 2). Here, overexpression of miR-92a
395 resulted in improved viability in late culture.
396
397 The fold change in miR levels, measured via RT-qPCR, was expressed relative to endogenous
398 expression in a control culture with transient transfection of apLifeAct-miRFP703 plasmid
399 (Figure 4c). Approximately a 2-fold difference in expression of let-7a, miR-21, and miR-92a was
400 observed on day 4 of culture, which is well within the range generally required for phenotypic
401 changes (Mestdagh et al., 2009).
402
403 Taken together, these results suggest novel pro- and anti-apoptotic roles for highly-expressed
404 CHO EV miR cargo in target CHO cells. The let-7a data suggest a potential pro-apoptotic
405 function for CHO EVs produced under ammonia/osmotic stress conditions (which upregulate
406 let-7a cargo levels). The miR-92a data suggest a potential anti-apoptotic function for CHO EVs
407 produced in unstressed, exponential-phase cultures (which upregulate miR-92a cargo levels).
408 Indeed, it is possible that miR-92a action plays a role in the protective effects of CHO EVs
409 reported in other studies (Han & Rhee, 2018; Takagi et al., 2021). The miR-21 data in this study
410 were unexpected, because, as noted previously, miR-21 has repeatedly been found to promote
411 growth and viability of other cell types.
412
413 **4. DISCUSSION:**
414 In this study, we measured total miR and protein levels on a stoichiometric ("per-EV") basis,
415 and then used RT-PCR to quantify the presence of total miR and protein cargo, as well as key

individual miRs. Total miR levels were significantly higher in CHO EVs from stressed cultures (Fig 1c), even as individual miR levels were often significantly lower (Fig 3a). This finding suggests that the bulk of the total miR content in CHO EVs from stressed cultures are *not* composed of solely the five miRs identified in standard cultures during exponential phase and investigated individually here (i.e. miR-92a, miR-21, miR-25, let-7c, miR-23a). Indeed, previous RNA sequencing of the osmotic and ammonia stressed cultures supports this, as the identities of the most abundant miRs in CHO EVs differ when parent cells are exposed to stress (Belliveau & Papoutsakis, 2023). We would expect a similar finding following the application of lactate stress. The apparent decrease in specific miRs studied here alongside the observed increase in bulk miR content over time suggests a dynamic miR landscape throughout culture that may be responsive to the culture environment. We hypothesize that the specific miRs identified previously with RNAseq from exponential phase, standard cultures support cells during this phase and in this environment. As the culture ages or stresses are added, our data suggests that the miR landscape also shifts where the previously identified miRs are no longer in high abundance. It is unsurprising that the miR landscape during exponential phase, standard cultures is not the same as during stationary or death phase and in stressed cultures. In our observations that the bulk miR content increases with culture age, we hypothesize that other unidentified miRs are increasing in abundance and future investigations into the CHO EV miR landscape will identify the specific miR content.

Similarly, we expect that RNA sequencing of CHO EVs from different growth phases would detect distinct miR profiles (relative to CHO EVs from day 3 culture) (C. Keysberg et al., 2021),

438 since CHO EVs under these conditions carry more total miR (Fig 1a) despite an apparent
439 downward trend in individual miR levels during early culture (Fig 2a). The stoichiometric
440 analysis of per-EV miR and protein levels presented in this study is unique in CHO EV research,
441 which has so far been limited to descriptions of relative RNA levels informed by RNA
442 sequencing data.
443
444 The exceptionally high enrichment of miR observed in the RT-PCR data, would logically be
445 interpreted to mean that the parent cells may achieve specific biological goals by this
446 enrichment. Since the large EVs are largely budding off the cytoplasmic membrane, the sorting
447 mechanism of miRs into large EVs likely enriches specific miRs in high concentrations and also
448 result in high concentrations of specific miRs near the cytoplasmic membrane.
449
450 Notably, this study represents the first analysis of the impact of lactate stress on CHO EV cargo.
451 Although the lactate concentrations employed in this study did not have a significant impact of
452 cell growth or viability, miR and protein levels in EVs were certainly affected. Lactate appears
453 similar to ammonia in terms of its effect on miR and protein cargo, and its impact extends
454 beyond its osmotic effects, which were controlled for by a 20 mOsm/L NaCl treatment (i.e., the
455 "osmotic control").
456
457 Considerations of analyzing RNAs associated with EV-free proteins that may co-precipitate
458 during ultracentrifugation was addressed in Turchinovich et al (Turchinovich, Weiz, Langheinz,
459 & Burwinkel, 2011), where it was demonstrated that microRNAs in cell culture media remain in

suspension after ultracentrifugation at 110,000 *g*. Here we used an ultracentrifugation speed of 28,000 *g*. There is currently no consensus protocol for RNase/protease treatment of EVs with a wide range of publications not RNase and/or protease treating EVs (Bellingham, Coleman, & Hill, 2012; Busch et al., 2022; Christoph Keysberg et al., 2021; Perez-Boza, Lion, & Struman, 2018). Alternatively, papers that do report using RNase treatment protocols use a wide range of RNase concentrations between 0.004 – 0.4 mg/mL (Bracht et al., 2021; Gutierrez Garcia et al., 2020; Lunavat et al., 2015; Valadi et al., 2007). A major concern of RNase treatment of EVs is inhibiting the RNases before EV lysis for RNA extraction. An additional issue arising from RNase treatment of EVs was documented in a previous publication from our lab, where we demonstrated that RNase treatment of EVs destroyed the native EV RNAs (Jiang, Kao, & Papoutsakis, 2017) because RNAses are taken up by cells and membrane vesicles. We had used RNAse treatment to decimate the native RNA cargo in order to load EVs with synthetic cargo. Thus, in our opinion and based on our experimental data, RNAse treatment is not an option for RNA analysis of EVs. Finally,, microRNAs found extracellularly are mostly bound to Ago2 proteins from lysed cells, which when bound to microRNAs is resistant to protease treatments (Elkayam et al., 2012; Turchinovich et al., 2011).

This study also explored the role of three specific miRs (let-7a, miR-21, and miR-92a) on cell growth, viability, and apoptosis in CHO cultures across growth phases. In transiently overexpressing let-7a, there was an observed decrease in cell growth and viability. There was no impact to cell growth in cultures transfected with the miR-92a plasmid and there was an observed increase in viability of these cultures on days 2 and 8. Cultures transfected with the

miR-21 plasmid did not demonstrate improved cell growth or viability (such improvement was expected, based on literature reports), with decreases in viability only on day 6 of culture. This result was somewhat surprising, and miR-21 has been associated with improved growth and viability in other cell types (Feng & Tsao, 2016; Krichevsky & Gabriely, 2009; Liu et al., 2014; Thabet et al., 2020; Yang et al., 2019).

These results suggest, for the first time, potential functions for the common miR cargoes carried by CHO EVs from stressed and unstressed cultures. Namely, let-7b (common in CHO EVs from stressed cultures) may induce CHO cell apoptosis, while miR-92a (common in CHO EVs from unstressed, exponential-phase cultures) may promote CHO cell survival. A more robust study stably overexpressing these miRs in CHO cells will be required to fully understand the role these miRs have on industrially-relevant parameters such as cell growth, viability, apoptosis, titer, and product quality (Bazaz et al., 2023; Leroux et al., 2021). Studies have revealed that specific combinations of miRs can result in phenotypic changes (Cursons et al., 2018; Kao et al., 2022), suggesting that the highly abundant miRs identified in CHO EVs may need to be examined in combination in order to identify any potential phenotypes.

The practical implications of this study are twofold. Differential miR and protein cargo loading suggest a use for CHO EVs as a culture diagnostic tool; indeed, the use of EV concentration as a metric for CHO culture health has already been demonstrated (Zavec et al., 2016). Both RT-PCR and our Qubit (total miR) and Bradford protein assays provide proof-of-concept for the relatively quick and simple evaluation of EV cargo. In several cases, these assays not only

identify the presence of stress, but also differentiate between types of stress (i.e., ammonia or lactate vs. osmotic stress). Some EV cargo characteristics—specifically, total miR and miR-92a/let-7c levels—could even serve to differentiate between different levels of the same stress (i.e., 20 mOsm/L and 120 mOsm/L osmotic stress). Beyond their potential as a diagnostic tool, CHO EVs offer an efficient miR (or protein) delivery system that does not require disruption of the plasma membrane or complex genetic engineering. Manipulating cellular phenotype via miR is particularly appealing for CHO culture, as miRs do not compete with the translational machinery used in protein production (Muller, Katinger, & Grillari, 2008). In this vein, this study reports novel findings regarding the pro- or anti-apoptotic functions (in CHO cells) of let-7a, miR-21, and miR-92a, and also provides a framework for understanding the age/stress conditions that produce CHO EVs with high or low levels of certain miRs.

Future research should investigate the identities of the specific protein chaperones responsible for altered EV cargo loading under stress. Additionally, though miR-92a and miR-21 are highly expressed by CHO EVs from early exponential phase culture and let-7a is highly expressed by CHO EVs produced under stress (Belliveau & Papoutsakis, 2023), these miRs are by no means the only cargo capable of inducing phenotype changes in target cells. The roles of other miRs—especially those present at high levels in EVs from stress conditions—must be evaluated. At some point, it will be necessary to conduct RNA sequencing (and possibly proteomic analysis) of CHO EVs produced under lactate stress and in lag- and stationary-phase culture, as we predict the presence of novel EV miR profiles in these conditions. In sum, our research initiates the long

process of linking CHO EV cargo with CHO EV function, suggesting exciting applications for CHO EVs as both diagnostic tools and culture therapeutics.

AUTHORSHIP CONTRIBUTIONS:

JB, WT and ETP designed the study and analyzed the data. JB and WT carried out the experiments. JB, WT and ETP wrote the manuscript. JB and WT should be considered joint first author.

CONFLICTS OF INTEREST:

The authors declare no conflicts of interest.

ACKNOWLEDGMENTS

The authors acknowledge the support of this work by Merck & Co., Inc. and the Advanced Mammalian Biomanufacturing Innovation Center (AMBIC) supported in part by the US National Science Foundation (NSF, Grant number 1624698) and industrial members of the Center, and notably Millipore Sigma and Sartorius. Will Thompson also acknowledges partial support by a US Department of Education GAANN Fellowship (Grant number P200A210065).

DATA AVAILABILITY:

The data used to support the findings of this study are available from the corresponding author upon reasonable request.

548

549 **REFERENCES:**

550 Anand, S., Samuel, M., Kumar, S., & Mathivanan, S. (2019). Ticket to a bubble ride: Cargo
551 sorting into exosomes and extracellular vesicles. *Biochim Biophys Acta Proteins*
552 *Proteom, 1867*(12), 140203. doi:10.1016/j.bbapap.2019.02.005

553 Bazaz, M., Adeli, A., Azizi, M., Karimipoor, M., Mahboudi, F., & Davoudi, N. (2023).
554 Overexpression of miR-32 in Chinese hamster ovary cells increases production of Fc-
555 fusion protein. *AMB Express, 13*(1), 45. doi:10.1186/s13568-023-01540-z

556 Bellingham, S. A., Coleman, B. M., & Hill, A. F. (2012). Small RNA deep sequencing reveals a
557 distinct miRNA signature released in exosomes from prion-infected neuronal cells.
558 *Nucleic Acids Research, 40*(21), 10937-10949. doi:10.1093/nar/gks832

559 Belliveau, J., & Papoutsakis, E. T. (2022). Extracellular vesicles facilitate large-scale dynamic
560 exchange of proteins and RNA among cultured Chinese hamster ovary and human cells.
561 *Biotechnol Bioeng, 119*(5), 1222-1238. doi:10.1002/bit.28053

562 Belliveau, J., & Papoutsakis, E. T. (2022). Extracellular vesicles facilitate large-scale dynamic
563 exchange of proteins and RNA among cultured Chinese hamster ovary and human cells.
564 *Biotechnology and Bioengineering, 119*(5), 1222-1238. doi:10.1002/bit.28053

565 Belliveau, J., & Papoutsakis, E. T. (2023). The microRNomes of Chinese hamster ovary (CHO)
566 cells and their extracellular vesicles, and how they respond to osmotic and ammonia
567 stress. *Biotechnol Bioeng, 120*(9), 2700-2716. doi:10.1002/bit.28356

Bracht, J. W. P., Gimenez-Capitan, A., Huang, C. Y., Potie, N., Pedraz-Valdunciel, C., Warren, S., . . . Molina-Vila, M. A. (2021). Analysis of extracellular vesicle mRNA derived from plasma using the nCounter platform. *Sci Rep, 11*(1), 3712. doi:10.1038/s41598-021-83132-0

Busch, D. J., Zhang, Y., Kumar, A., Huhn, S. C., Du, Z., & Liu, R. (2022). Identification of RNA content of CHO-derived extracellular vesicles from a production process. *Journal of Biotechnology, 348*, 36-46. doi:10.1016/j.jbiotec.2022.03.004

Chevillet, J. R., Kang, Q., Ruf, I. K., Briggs, H. A., Vojtech, L. N., Hughes, S. M., . . . Tewari, M. (2014). Quantitative and stoichiometric analysis of the microRNA content of exosomes. *Proc Natl Acad Sci U S A, 111*(41), 14888-14893. doi:10.1073/pnas.1408301111

Cho, K. J., Song, J., Oh, Y., & Lee, J. E. (2015). MicroRNA-Let-7a regulates the function of microglia in inflammation. *Mol Cell Neurosci, 68*, 167-176. doi:10.1016/j.mcn.2015.07.004

Corrado, C., Barreca, M. M., Zichittella, C., Alessandro, R., & Conigliaro, A. (2021). Molecular Mediators of RNA Loading into Extracellular Vesicles. *Cells, 10*(12), 3355. doi:10.3390/cells10123355

Cursons, J., Pillman, K. A., Scheer, K. G., Gregory, P. A., Foroutan, M., Hediyeh-Zadeh, S., . . . Davis, M. J. (2018). Combinatorial Targeting by MicroRNAs Co-ordinates Post-transcriptional Control of EMT. *Cell Syst, 7*(1), 77-91 e77. doi:10.1016/j.cels.2018.05.019

Dellar, E. R., Hill, C., Melling, G. E., Carter, D. R. F., & Baena-Lopez, L. A. (2022). Unpacking extracellular vesicles: RNA cargo loading and function. *Journal of Extracellular Biology, 1*(5), e40. doi:10.1002/jex2.40

589 Elkayam, E., Kuhn, C. D., Tocilj, A., Haase, A. D., Greene, E. M., Hannon, G. J., & Joshua-Tor, L.
590 (2012). The structure of human argonaute-2 in complex with miR-20a. *Cell, 150*(1), 100-
591 110. doi:10.1016/j.cell.2012.05.017
592 Fabbiano, F., Corsi, J., Gurrieri, E., Trevisan, C., Notarangelo, M., & D'Agostino, V. G. (2020). RNA
593 packaging into extracellular vesicles: An orchestra of RNA-binding proteins? *J Extracell*
594 *Vesicles, 10*(2), e12043. doi:10.1002/jev2.12043
595 Feng, Y. H., & Tsao, C. J. (2016). Emerging role of microRNA-21 in cancer. *Biomed Rep, 5*(4), 395-
596 402. doi:10.3892/br.2016.747
597 George, S. K., Laukova, L., Weiss, R., Semak, V., Fendl, B., Weiss, V. U., . . . Weber, V. (2021).
598 Comparative Analysis of Platelet-Derived Extracellular Vesicles Using Flow Cytometry
599 and Nanoparticle Tracking Analysis. *Int J Mol Sci, 22*(8), 3839. doi:10.3390/ijms22083839
600 Gutierrez Garcia, G., Galicia Garcia, G., Zalapa Soto, J., Izquierdo Medina, A., Rotzinger-
601 Rodriguez, M., Casas Aguilar, G. A., . . . Aguilar-Hernandez, M. M. (2020). Analysis of RNA
602 yield in extracellular vesicles isolated by membrane affinity column and differential
603 ultracentrifugation. *PLoS One, 15*(11), e0238545. doi:10.1371/journal.pone.0238545
604 Han, S., & Rhee, W. J. (2018). Inhibition of apoptosis using exosomes in Chinese hamster ovary
605 cell culture. *Biotechnol Bioeng, 115*(5), 1331-1339. doi:10.1002/bit.26549
606 Jiang, J., Kao, C. Y., & Papoutsakis, E. T. (2017). How do megakaryocytic microparticles target
607 and deliver cargo to alter the fate of hematopoietic stem cells? *J Control Release, 247*, 1-
608 18. doi:10.1016/j.jconrel.2016.12.021
609 Kao, C. Y., Jiang, J. L., Thompson, W., & Papoutsakis, E. T. (2022). miR-486-5p and miR-22-3p
610 Enable Megakaryocytic Differentiation of Hematopoietic Stem and Progenitor Cells

without Thrombopoietin. *International Journal of Molecular Sciences, 23*(10), 5355. doi:10.3390/ijms23105355

Kao, C. Y., & Papoutsakis, E. T. (2019). Extracellular vesicles: exosomes, microparticles, their parts, and their targets to enable their biomanufacturing and clinical applications. *Curr Opin Biotechnol, 60*, 89-98. doi:10.1016/j.copbio.2019.01.005

Keysberg, C., Hertel, O., Schelletter, L., Busche, T., Sochart, C., Kalinowski, J., . . . Noll, T. (2021). Exploring the molecular content of CHO exosomes during bioprocessing. *Applied Microbiology and Biotechnology, 105*(9), 3673-3689. doi:10.1007/s00253-021-11309-8

Keysberg, C., Hertel, O., Schelletter, L., Busche, T., Sochart, C., Kalinowski, J., . . . Noll, T. (2021). Exploring the molecular content of CHO exosomes during bioprocessing. *Appl Microbiol Biotechnol, 105*(9), 3673-3689. doi:10.1007/s00253-021-11309-8

Kondratov, K., Nikitin, Y., Fedorov, A., Kostareva, A., Mikhailovskii, V., Isakov, D., . . . Golovkin, A. (2020). Heterogeneity of the nucleic acid repertoire of plasma extracellular vesicles demonstrated using high-sensitivity fluorescence-activated sorting. *J Extracell Vesicles, 9*(1), 1743139. doi:10.1080/20013078.2020.1743139

Krichevsky, A. M., & Gabriely, G. (2009). miR-21: a small multi-faceted RNA. *J Cell Mol Med, 13*(1), 39-53. doi:10.1111/j.1582-4934.2008.00556.x

Kumar, N., Gupta, D., Kumar, S., Maurya, P., Tiwari, A., Mathew, B., . . . Chaudhuri, S. (2016). Exploring Packaged Microvesicle Proteome Composition of Chinese Hamster Ovary Secretome. *Journal of Bioprocessing & Biotechniques, 6*(4), 1000274.

631 Leidal, A. M., & Debnath, J. (2020). Unraveling the mechanisms that specify molecules for
632 secretion in extracellular vesicles. *Methods, 177*, 15-26.
633 doi:10.1016/j.ymeth.2020.01.008
634 Leroux, A. C., Bartels, E., Winter, L., Mann, M., Otte, K., & Zehe, C. (2021). Transferability of
635 miRNA-technology to bioprocessing: Influence of cultivation mode and media.
636 *Biotechnol Prog, 37*(2), e3107. doi:10.1002/btpr.3107
637 Liu, Y., Wang, X., Yang, D., Xiao, Z., & Chen, X. (2014). MicroRNA-21 affects proliferation and
638 apoptosis by regulating expression of PTEN in human keloid fibroblasts. *Plast Reconstr*
639 *Surg, 134*(4), 561e-573e. doi:10.1097/PRS.0000000000000577
640 Livak, K., & Schmittgen, T. (2001). Analysis of relative gene expression data using real-time
641 quantitative PCR and the 2(-Delta Delta C(T)) Method. *Methods, 25*(4), 402-408.
642 doi:10.1006/meth.2001.1262
643 Loh, W. P., Yang, Y., & Lam, K. P. (2017). miR-92a enhances recombinant protein productivity in
644 CHO cells by increasing intracellular cholesterol levels. *Biotechnology Journal, 12*(4),
645 1600488. doi:10.1002/biot.201600488
646 Lunavat, T. R., Cheng, L., Kim, D. K., Bhadury, J., Jang, S. C., Lasser, C., . . . Lotvall, J. (2015). Small
647 RNA deep sequencing discriminates subsets of extracellular vesicles released by
648 melanoma cells--Evidence of unique microRNA cargos. *RNA Biol, 12*(8), 810-823.
649 doi:10.1080/15476286.2015.1056975
650 Mestdagh, P., Van Vlierberghe, P., De Weer, A., Muth, D., Westermann, F., Speleman, F., &
651 Vandesompele, J. (2009). A novel and universal method for microRNA RT-qPCR data
652 normalization. *Genome Biol, 10*(6), R64. doi:10.1186/gb-2009-10-6-r64

Mogilyansky, E., & Rigoutsos, I. (2013). The miR-17/92 cluster: a comprehensive update on its genomics, genetics, functions and increasingly important and numerous roles in health and disease. *Cell Death Differ, 20*(12), 1603-1614. doi:10.1038/cdd.2013.125

Muller, D., Katinger, H., & Grillari, J. (2008). MicroRNAs as targets for engineering of CHO cell factories. *Trends Biotechnol, 26*(7), 359-365. doi:10.1016/j.tibtech.2008.03.010

O'Brien, K., Breyne, K., Ughetto, S., Laurent, L. C., & Breakefield, X. O. (2020). RNA delivery by extracellular vesicles in mammalian cells and its applications. *Nat Rev Mol Cell Biol, 21*(10), 585-606. doi:10.1038/s41580-020-0251-y

Perez-Boza, J., Lion, M., & Struman, I. (2018). Exploring the RNA landscape of endothelial exosomes. *RNA, 24*(3), 423-435. doi:10.1261/rna.064352.117

Perge, P., Butz, H., Pezzani, R., Bancos, I., Nagy, Z., Paloczi, K., . . . Igaz, P. (2017). Evaluation and diagnostic potential of circulating extracellular vesicle-associated microRNAs in adrenocortical tumors. *Sci Rep, 7*(1), 5474. doi:10.1038/s41598-017-05777-0

Raposo, G., & Stoorvogel, W. (2013). Extracellular vesicles: exosomes, microvesicles, and friends. *J Cell Biol, 200*(4), 373-383. doi:10.1083/jcb.201211138

Shigoka, M., Tsuchida, A., Matsudo, T., Nagakawa, Y., Saito, H., Suzuki, Y., . . . Kuroda, M. (2010). Deregulation of miR-92a expression is implicated in hepatocellular carcinoma development. *Pathology International, 60*(5), 351-357. doi:10.1111/j.1440-1827.2010.02526.x

Stevanato, L., Thanabalasundaram, L., Vysokov, N., & Sinden, J. D. (2016). Investigation of Content, Stoichiometry and Transfer of miRNA from Human Neural Stem Cell Line Derived Exosomes. *PLoS One, 11*(1), e0146353. doi:10.1371/journal.pone.0146353

675 Takagi, M., Jimbo, S., Oda, T., Goto, Y., & Fujiwara, M. (2021). Polymer fraction including
676 exosomes derived from Chinese hamster ovary cells promoted their growth during
677 serum-free repeated batch culture. *J Biosci Bioeng, 131*(2), 183-189.
678 doi:10.1016/j.jbiosc.2020.09.011
679 Thabet, E., Yusuf, A., Abdelmonsif, D. A., Nabil, I., Mourad, G., & Mehanna, R. A. (2020).
680 Extracellular vesicles miRNA-21: a potential therapeutic tool in premature ovarian
681 dysfunction. *Mol Hum Reprod, 26*(12), 906-919. doi:10.1093/molehr/gaaa068
682 Thery, C., Witwer, K. W., Aikawa, E., Alcaraz, M. J., Anderson, J. D., Andriantsitohaina, R., . . .
683 Zuba-Surma, E. K. (2018). Minimal information for studies of extracellular vesicles 2018
684 (MISEV2018): a position statement of the International Society for Extracellular Vesicles
685 and update of the MISEV2014 guidelines. *J Extracell Vesicles, 7*(1), 1535750.
686 doi:10.1080/20013078.2018.1535750
687 Tsang, W. P., & Kwok, T. T. (2008). Let-7a microRNA suppresses therapeutics-induced cancer
688 cell death by targeting caspase-3. *Apoptosis, 13*(10), 1215-1222. doi:10.1007/s10495-
689 008-0256-z
690 Turchinovich, A., Weiz, L., Langheinz, A., & Burwinkel, B. (2011). Characterization of
691 extracellular circulating microRNA. *Nucleic Acids Research, 39*(16), 7223-7233.
692 doi:10.1093/nar/gkr254
693 Valadi, H., Ekstrom, K., Bossios, A., Sjostrand, M., Lee, J. J., & Lotvall, J. O. (2007). Exosome-
694 mediated transfer of mRNAs and microRNAs is a novel mechanism of genetic exchange
695 between cells. *Nat Cell Biol, 9*(6), 654-659. doi:10.1038/ncb1596

van Niel, G., D'Angelo, G., & Raposo, G. (2018). Shedding light on the cell biology of extracellular vesicles. *Nature Reviews: Molecular Cell Biology, 19*, 213-228. doi:10.1038/nrm.2017.125

Wei, Z., Batagov, A. O., Schinelli, S., Wang, J., Wang, Y., El Fatimy, R., . . . Krichevsky, A. M. (2017). Coding and noncoding landscape of extracellular RNA released by human glioma stem cells. *Nat Commun, 8*(1), 1145. doi:10.1038/s41467-017-01196-x

Xu, G. Q., Li, L. H., Wei, J. N., Xiao, L. F., Wang, X. T., Pang, W. B., . . . Song, G. H. (2019). Identification and profiling of microRNAs expressed in oral buccal mucosa squamous cell carcinoma of Chinese hamster. *Sci Rep, 9*(1), 15616. doi:10.1038/s41598-019-52197-3

Yang, Y. C., Liu, G. J., Yuan, D. F., Li, C. Q., Xue, M., & Chen, L. J. (2019). Influence of exosome-derived miR-21on chemotherapy resistance of esophageal cancer. *Eur Rev Med Pharmacol Sci, 23*(4), 1513-1519. doi:10.26355/eurrev_201902_17109

Zavec, A. B., Kralj-Iglič, V., Brinc, M., Trček, T. F., Kuzman, D., Schweiger, A., & Anderluh, G. (2016). Extracellular vesicles concentration is a promising and important parameter for industrial bioprocess monitoring. *Biotechnology Journal, 11*(5), 603-609. doi:10.1002/biot.201500049

Zhao, W., Hu, J. X., Hao, R. M., Zhang, Q., Guo, J. Q., Li, Y. J., . . . Xie, S. Y. (2018). Induction of microRNA-let-7a inhibits lung adenocarcinoma cell growth by regulating cyclin D1. *Oncology Reports*. doi:10.3892/or.2018.6593

Zhou, C., Shen, L., Mao, L., Wang, B., Li, Y., & Yu, H. (2015). miR-92a is upregulated in cervical cancer and promotes cell proliferation and invasion by targeting FBXW7. *Biochem Biophys Res Commun, 458*(1), 63-69. doi:10.1016/j.bbrc.2015.01.066

718

719

Figure captions:

Figure 1. Total miR and protein levels in CHO EVs. Total **(a)** miR and **(b)** protein levels in CHO EVs were measured at different points in culture and normalized to CHO EV quantity. Total **(c)** miR and **(d)** protein levels in CHO EVs produced under osmotic, ammonia, and lactate stress were measured and normalized to CHO EV quantity. Error bars represent the standard error of the mean (SEM) of 3 replicates. Significance was determined with unpaired Student's t-test, * for $p<0.05$, ** for $p<0.01$.

Figure 2. Individual miR levels in CHO EVs and CHO cells at various timepoints in culture. The levels of five abundant miRs were individually measured in **(a)** CHO EVs and **(b)** CHO cells at different points in culture via RT-PCR. Error bars represent the standard error of the mean (SEM) of 3 replicates. Significance was determined with unpaired Student's t-test, * for $p<0.05$, ** for $p<0.01$.

Figure 3. Individual miR levels in CHO EVs and CHO cells from stressed cultures. The levels of five abundant miRs were individually measured in **(a)** CHO EVs and **(b)** CHO cells from stress-treated day 3 cultures via RT-PCR. The bars in (b) represent fold change relative to unstressed control cell miR levels. Error bars represent the standard error of the mean (SEM) of 3-4 replicates. Significance was determined with unpaired Student's t-test. For significance relative to another stressed sample, * for $p<0.05$, ** for $p<0.01$; for significance relative to the unstressed control, † for $p<0.05$.

Figure 4. Transient expression of let-7a, miR-21, and miR-92a. (a) Cell growth curve of cells transiently expressing let-7a, miR-21, or miR-92a compared to the control (transient transfection of pLifeAct-miRFP703). **(b)** Annexin V/7AAD flow cytometry viability assay of cultures transiently transfected with the control plasmid (pLifeAct-miRFP703), let-7a plasmid, miR-21 plasmid, or miR-92a plasmid. Conditions where viability was significantly lower than the associated control are red. Conditions where viability was significantly greater than the associated control are green. **(c)** Fold change in cultures transiently expressing let-7a, miR-21, and miR-92a compared to the endogenous expression in the control culture (transient transfection of pLifeAct-miRFP703). Error bars represent the standard error of the mean (SEM) of 3-4 replicates. Significance relative to control was determined with unpaired Student's t-test, * for $p<0.05$, ** for $p<0.01$, *** for $p<0.001$.

Graphical Abstract

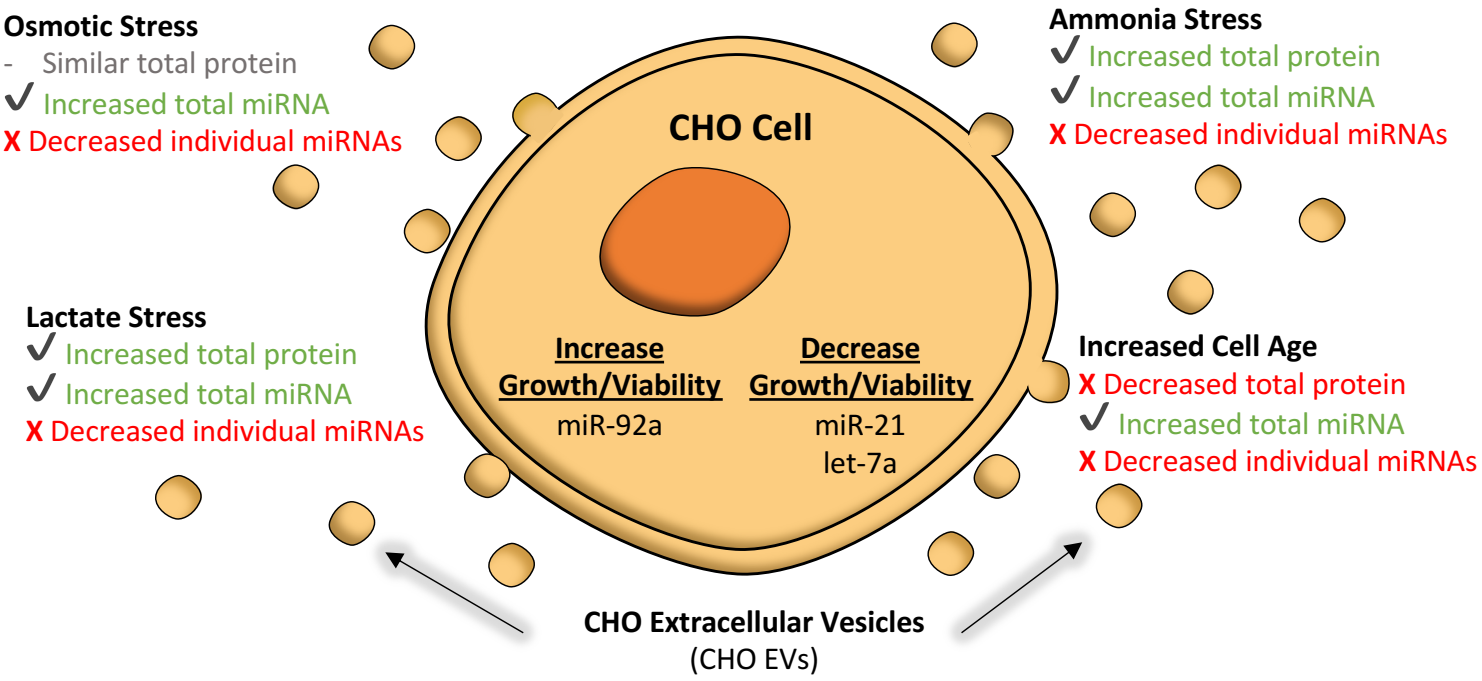

Figure 1

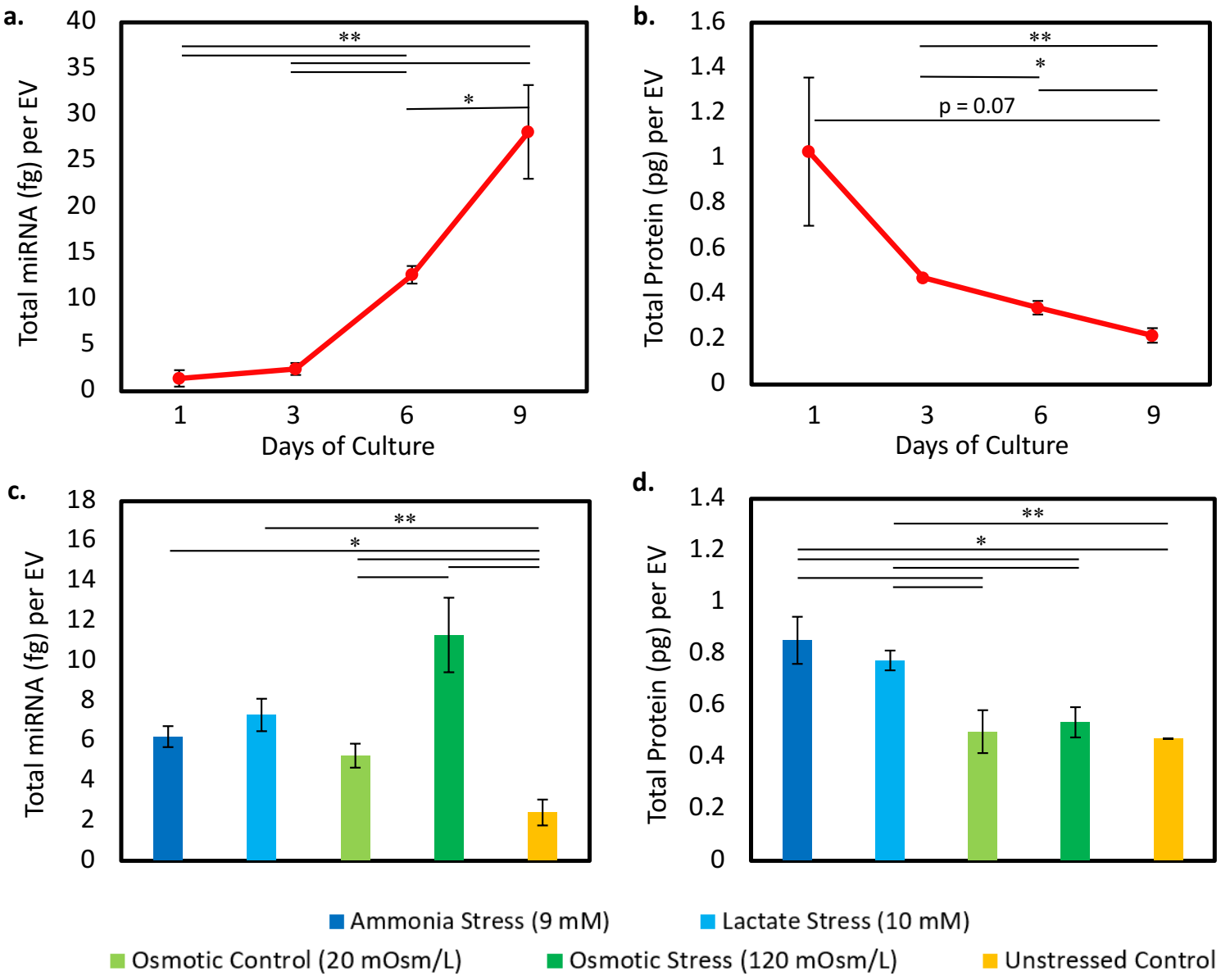
a.
Total miRNA (fg) per EV
Days of Culture
**
*
b.
Total Protein (pg) per EV
Days of Culture
**
*
p = 0.07
c.
Total miRNA (fg) per EV
**
*
d.
Total Protein (pg) per EV
**
*
Ammonia Stress (9 mM)
Lactate Stress (10 mM)
Osmotic Control (20 mOsm/L)
Osmotic Stress (120 mOsm/L)
Unstressed Control

Figure 2

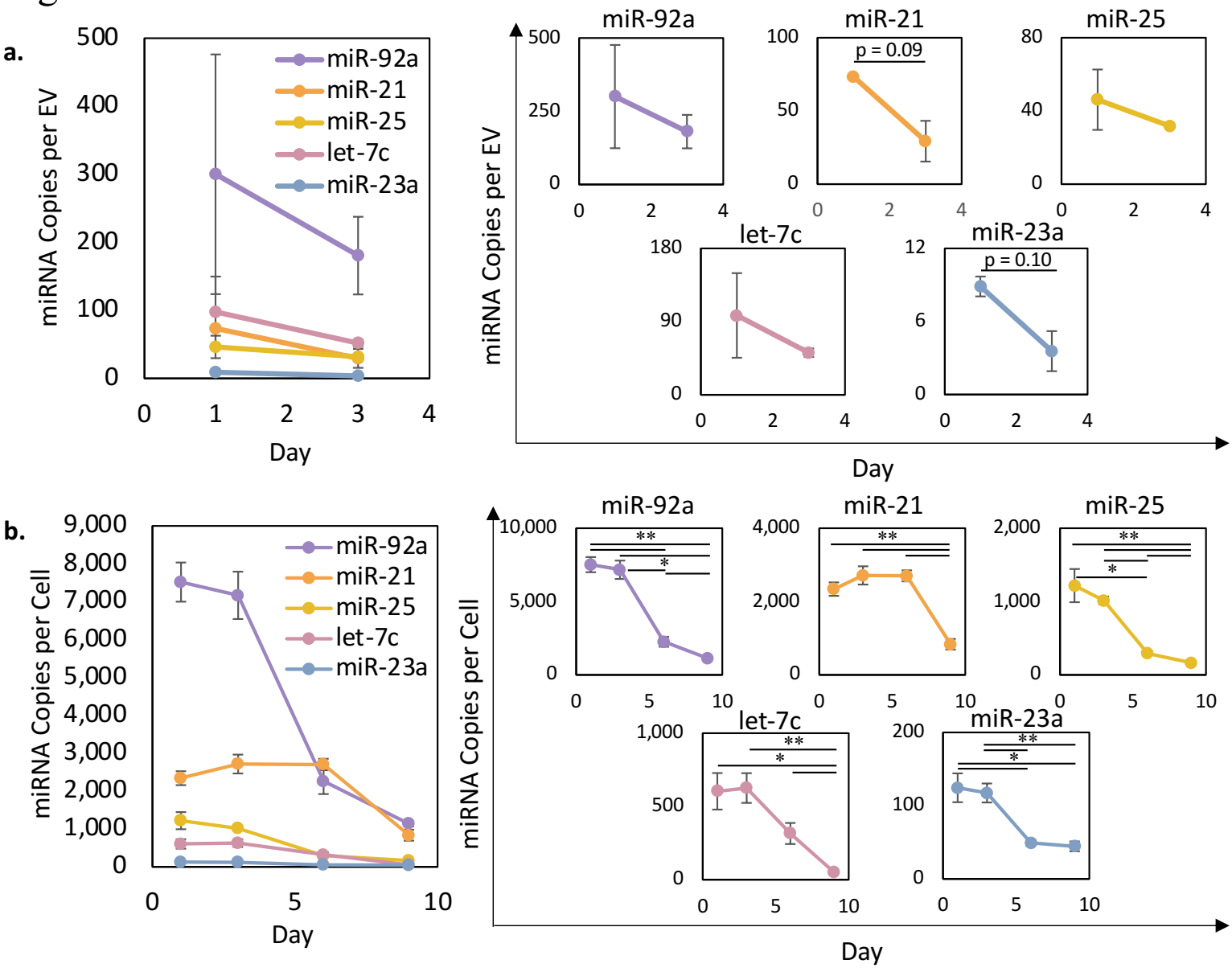
a.
miRNA Copies per EV
Day
miR-92a
miR-21
miR-25
let-7c
miR-23a
p = 0.09
p = 0.10
b.
miRNA Copies per Cell
Day
**
*

Figure 3

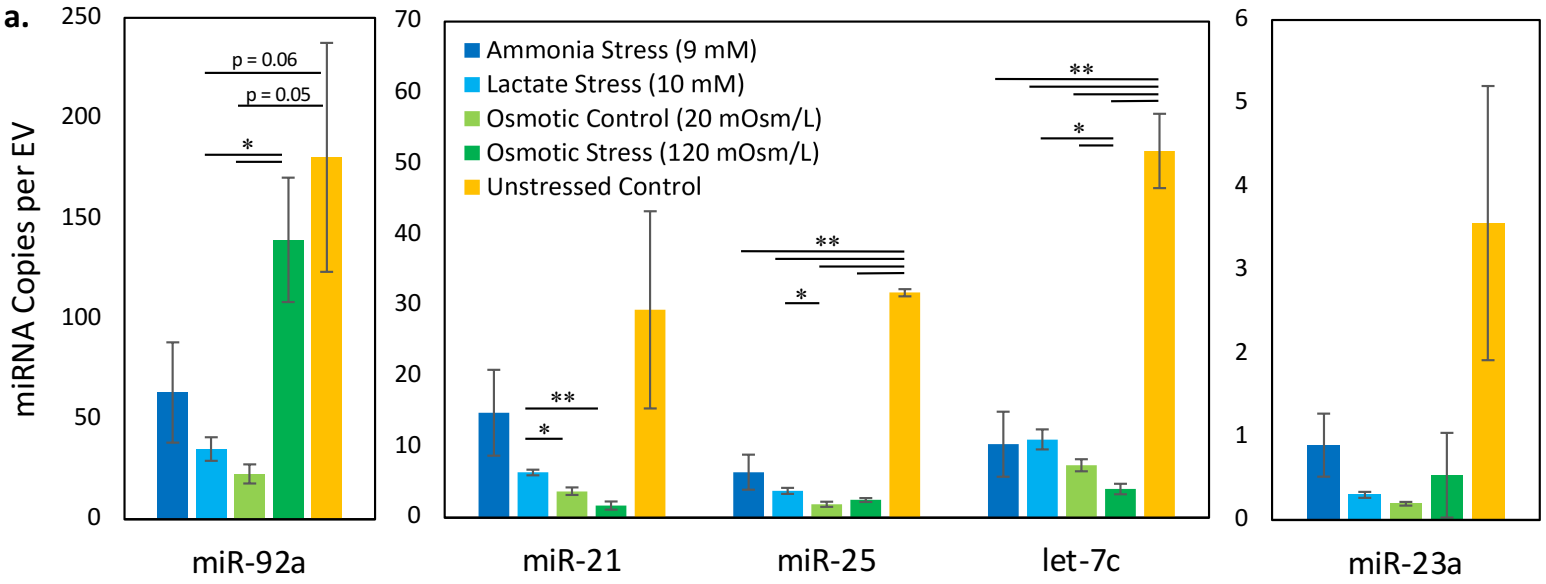
a.
miRNA Copies per EV
Ammonia Stress (9 mM)
Lactate Stress (10 mM)
Osmotic Control (20 mOsm/L)
Osmotic Stress (120 mOsm/L)
Unstressed Control
p = 0.06
p = 0.05
miR-92a
miR-21
miR-25
let-7c
miR-23a

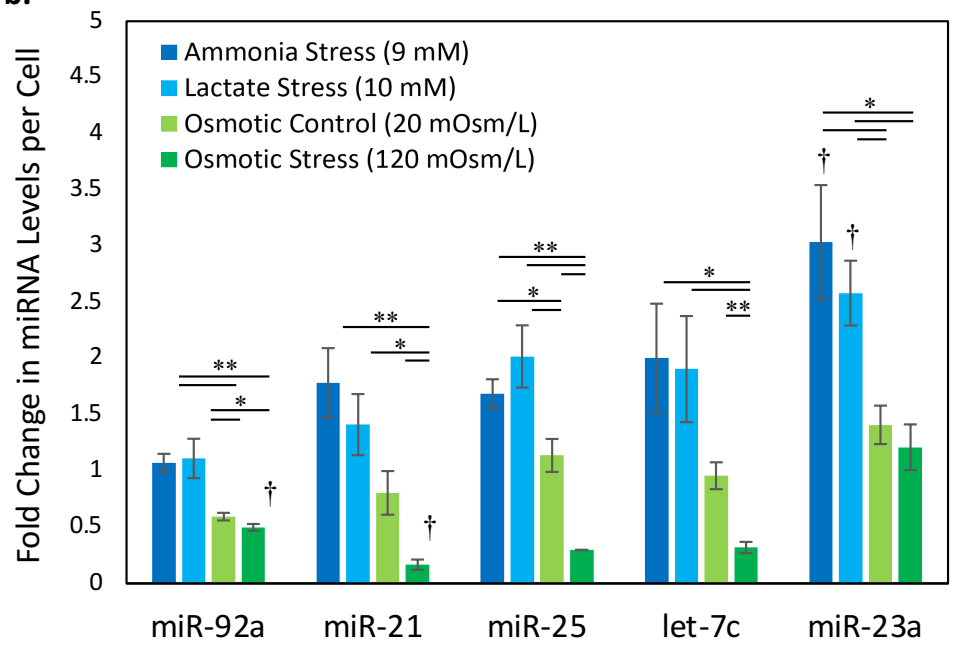
b.
Fold Change in miRNA Levels per Cell
Ammonia Stress (9 mM)
Lactate Stress (10 mM)
Osmotic Control (20 mOsm/L)
Osmotic Stress (120 mOsm/L)
miR-92a
miR-21
miR-25
let-7c
miR-23a

Figure 4

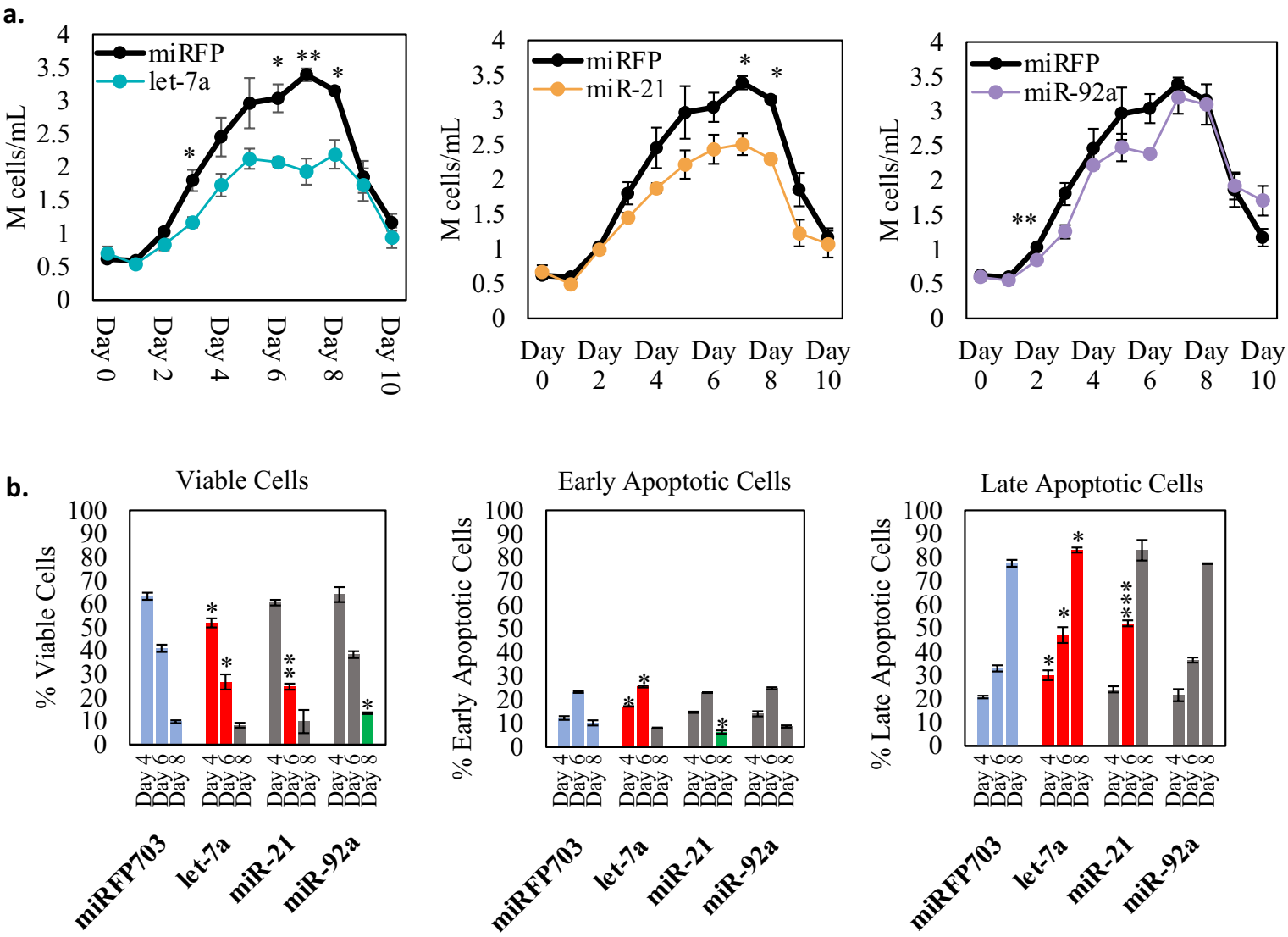
a.
M cells/mL
miRFP
let-7a
miR-21
miR-92a
Day 0
Day 2
Day 4
Day 6
Day 8
Day 10
b.
Viable Cells
Early Apoptotic Cells
Late Apoptotic Cells
% Viable Cells
% Early Apoptotic Cells
% Late Apoptotic Cells
miRFP703
let-7a
miR-21
miR-92a
c.
Fold Change
Day 4 Day 6 Day 8 Day 4 Day 6 Day 8 Day 4 Day 6 Day 8
let-7a
miR-21
miR-92a

Supplementary Materials for

Kinetic and functional analysis of abundant microRNAs in extracellular vesicles from normal and stressed cultures of Chinese Hamster Ovary (CHO) cells

Jessica Belliveau, [1,2,*] Will Thompson [1,2,*] and Eleftherios Terry Papoutsakis [1,2,3]

[1] Department of Chemical and Biomolecular Engineering, University of Delaware, Newark, Delaware, USA

[2] Delaware Biotechnology Institute, University of Delaware, Newark, Delaware, USA

[3] Department of Biological Sciences, University of Delaware, Newark, Delaware, USA

[*] Jessica Belliveau (ORCID # 0000-0003-3466-6428) and Will Thompson (ORCID #0000-0002-0014-1941) should be considered joint first author

Correspondence: Eleftherios Terry Papoutsakis, 590 Avenue 1743, Newark, DE 19713, USA. E-mail: epaps@udel.edu; Tel: +1-302-831-8376; ORCID # 0000-0002-1077-1277

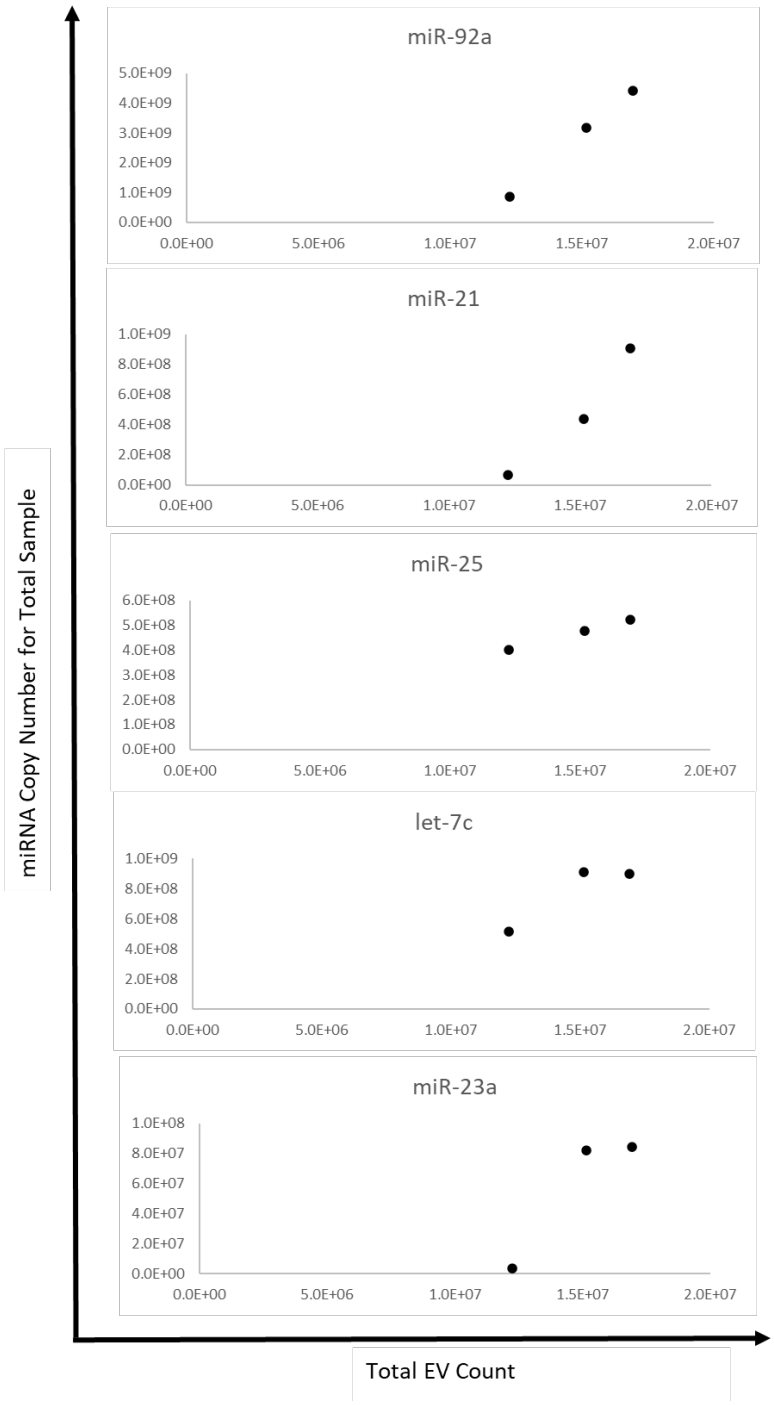

Figure S1. miRNA copy numbers increase linearly with EV count. For the control condition (day 3 EVs from "healthy," unstressed culture), total miRNA copies per sample are shown (normalized to miR-39 quantity) as a function of total EV count per sample. Sample volume, rather than EV count, was kept constant. Spike-in control cel-miR-39-3p (1 pmol/sample) was used to calculate copy numbers via the $2^{-\Delta\Delta CT}$ method. As expected, miRNA quantities increase roughly linearly with EV count, confirming the validity of the method. Each point represents PCR data for one biological replicate; each biological replicate is informed by three technical replicates. The data points in each plot were averaged to calculate the copies per EV of each miRNA; these average values are displayed in Figures 2a and 3a.